

GAMMA-RAY BURST SPECTRAL FEATURES: INTERPRETATION AS X-RAY EMISSION FROM A
PHOTOIONIZED PLASMAC. J. HAILEY¹, F. A. HARRISON² AND K. MORI¹*Accepted for publication in the Astrophysical Journal (Letters)*

ABSTRACT

Numerous reports have been made of features, either in emission or absorption, in the 10 - 1000 keV spectra of some gamma-ray bursts. Originally interpreted in the context of Galactic neutron star models as cyclotron line emission and $e^+ - e^-$ annihilation features, the recent demonstration that the majority of GRBs lie at cosmological distances make these explanations unlikely. In this letter, we adopt a relativistic fireball model for cosmological GRBs in which dense, metal rich blobs or filaments of plasma are entrained in the relativistic outflow. In the context of this model, we investigate the conditions under which broadband features, similar to those detected, can be observed. We find a limited region of parameter space capable of reproducing the observed GRB spectra. Finally, we discuss possible constraints further high-energy spectral observations could place on fireball model parameters.

Subject headings: binaries:close – cosmology:observations – gamma rays:bursts – stars:neutron

1. INTRODUCTION

Numerous detections have been reported of features, either in emission or absorption, in the spectra of some gamma-ray bursts (GRB). Absorption features below 100 keV were reported by Konus (Mazets *et al.* 1981), *HEAO A-1* (Hueter 1984), and *Ginga* (Murakami *et al.* 1988), and in addition Konus and other instruments have detected broad emission-like features at high energy (400 – 500 keV) in a few cases (e.g. Mazets *et al.* 1979, Teegarden & Cline 1980). The BATSE Spectroscopy Detectors (SD) on *CGRO* have recently reported 13 statistically significant line candidates, although some uncertainty in the contribution of systematics to the analysis make these detections uncertain (Briggs *et al.* 1999). For the most statistically significant BATSE candidate, GRB 930916, the feature appears as a broad bump between 41 and 51 keV (Briggs *et al.* 1999). Even if the BATSE features are not confirmed, the SD data cannot yet rule out the existence of features similar to those seen by *Ginga* in some fraction of GRBs (Band *et al.* 1996), and confirmation awaits more sensitive spectroscopic gamma-ray instruments.

Originally, these line features were interpreted in the context of Galactic neutron star models for the GRB progenitors. The low-energy absorption features were explained as cyclotron resonance lines in a $\sim 10^{12}$ Gauss magnetic field (Higdon & Lin- genfelter 1990, Fenimore *et al.* 1988), and the high-energy lines were postulated to be from $e^+ - e^-$ annihilation radiation gravitationally redshifted near the surface of a solar mass neutron star (e.g. Liang 1986). Recently, however, detection of redshifted absorption lines in the optical counterparts associated with two bursts (Metzger *et al.* 1997, Kulkarni *et al.* 1999), and emission lines from the galaxies associated with three others (Kulkarni *et al.* 1998, Djorgovski *et al.* 1998a, Djorgovski *et al.* 1998b) have confirmed cosmological distances for five GRBs. Although the BATSE data still allow a fraction of GRBs to be in a Galactic distribution (Loredo & Wasserman 1995), the majority of long GRBs must be cosmological. It is possible that the observed gamma-ray spectral features are associated with a subpopulation of Galactic GRB progenitors. However, given

the recent redshift and host galaxy observations this seems unlikely. It is therefore interesting to look for an explanation for these features in the context of cosmological GRB models.

Recently, Mészáros and Rees (1998) have discussed the possibility that the relativistic outflows associated with cosmological GRBs may entrain small blobs or filaments of dense, highly-ionized metal rich material that could give rise to broad features due to Fe K-edges in the GRB spectrum. For typical blob Lorenz factors of $\Gamma_b \sim 25 - 100$, Fe K-edges would give rise to isolated broad features in the 250 – 1000 keV band, similar perhaps to the high-energy lines observed by Konus. It would be difficult, however, to produce the line observed by *Ginga*, which have multiple features below 100 keV. In this letter, we accept the line detections as real, and investigate the possibility that the low-energy lines seen by *Ginga* could be produced by excitation and absorption in the predominantly Ne-like Fe-L complex and/or in outflows containing low-Z elements. As we show in §3, features similar to the *Ginga* lines can be produced both by O, Ne, Si-rich outflows, and by a combination of Fe and light elements. Finally, in the context of this model, we discuss the utility of broad band X- and gamma-ray spectroscopy for constraining fireball model parameters and the composition of the ejecta.

2. MODEL AND CALCULATIONS

In the model described by Mészáros and Rees (1998) (hereafter MR98), metal-enriched, high-density regions become entrained in the fireball, and are confined by the high ambient and ram pressure of the relativistic outflow. These small blobs or filaments, although a negligible fraction of the total outflow mass, can have a significant covering factor. Blobs with gas temperature comparable to the comoving photon temperature (~ 1 keV for typical fireball model parameters) would form photoionized plasmas with prominent line emission, similar to those found in many X-ray emitting sources. The plasma density would be high by most astrophysical standards, reaching $n_b \sim 10^{18} \text{ cm}^{-3}$ (assuming typical fireball parameters) for the case where the blob internal pressure balances the total external (magnetic and

¹Columbia Astrophysics Laboratory, Columbia University, New York, NY 10027²Space Radiation Laboratory and Division of Physics, Mathematics and Astronomy, California Institute of Technology, Pasadena, CA 91125

particle) pressure. These blobs would be accelerated by radiation or magneto-hydrodynamic pressure and would achieve a saturation bulk Lorentz factor well before reaching the emission region where internal shocks convert a significant fraction of the bulk kinetic energy into radiation ($r_{sh} \sim 10^{13}$ cm).

As described in MR98, several factors would broaden any spectral features from the dense photoionized plasma. If all blobs have the same bulk Lorentz factor, Γ_b , emission line features will be broadened due to contributions from regions with velocities that are at different angles to our line of sight, which will have different Doppler blue-shifts. In addition, the blobs may have a range of Lorentz factors, since those with low enough column would be accelerated to the velocity of the surrounding flow, whereas those with larger columns would reach slower terminal velocities. The range of Lorentz factors then depends on the range of blob sizes, which in turn depends on the details of the entrainment process and the extent to which instabilities break up the bigger blobs.

We have adopted this basic scenario described in MR98, and investigated the conditions under which low-energy features similar to those seen by *Ginga* can be formed. Our goal was to qualitatively reproduce multiple spectral features with a similar fraction of the total luminosity. It is important to note that the actual shape of the *Ginga* features is very sensitive to proper subtraction of the underlying continuum, and therefore on proper understanding of the instrument response. Given the imperfect knowledge of the *Ginga* response, varying assumptions about the continuum can cause the features to appear qualitatively different (Fenimore *et al.* 1988). We assume that the blobs are in pressure equilibrium with the surrounding medium (otherwise they would not be stable), and in addition, treat the optically thin regime only. Although the model itself does not impose any limit on the optical depth, the optically thin assumption represents the simplest case, where self-shielding and other time-dependent effects can be ignored.

We used the photoionization code, XSTAR (Kallman & Krolik 1995), to directly calculate the reprocessed spectrum and temperature of the photoionized material. As input to the code, we must specify the ionization parameter, $\Xi = L/(n_b r^2)$ (here L is the luminosity, n_b the blob particle density, and r the blob size). In the comoving frame, $\Xi = L/n_b r^2 \Gamma_b^2$ (MR98). Additional inputs are the ionizing spectrum and relative elemental abundances. For the ionization parameter, we investigated the range $\Xi = 100 - 1000$ consistent with the fireball model parameters of MR98. Similarly we considered the relevant range $\Gamma_b = 25 - 100$. We assume a power-law ionizing spectrum with energy index α , varied between 0.1 and 0.5, consistent with the average continuum spectrum early in the burst. Few constraints can be placed on the relative elemental abundances, since for neutron star mergers or hypernova scenarios, little is known about the composition of the surface. We have therefore investigated a range for the abundant elements O, Ne, Si, and Fe.

The XSTAR output, after ionization equilibrium is established, consists of the blob temperature (in the comoving frame), the abundance of each ion, prominent lines and edges with location and magnitude, and the ratio of bolometric recombination line to continuum luminosity. Given the assumption of pressure equilibrium, the choice of Ξ fixes the blob temperature in the co-moving frame; $\Xi = 500T_7$, where $T = 10^7 T_7$ K (MR98, assuming an isotropic blob distribution). We discard as inconsistent any solutions that do not satisfy the required relationship between Ξ and T . We also consider a range of reprocessing rates (ratio of total recombination luminosity to total ionizing

luminosity), which we adjust in order to find solutions with a ratio of deposited luminosity in the broad features to total luminosity of a few percent, consistent with the *Ginga* observations. We keep only solutions that have total optical depth in the lines, $\tau \leq 1$, consistent with the optically thin assumption.

With the output from XSTAR, and the assumed reprocessing rate, we calculate an observed spectrum by blueshifting (by Γ_b), and broadening with the instrumental width and the (dominant) relativistic effect resulting from the variation of velocity projected along the line of sight. To determine the magnitude of the latter, we assume the Lorentz factor and the luminosity to be independent of time, and we integrate over the spherical emission surface, assuming the emitting material to be uniformly distributed. This results in a spectral smearing of $\sim 50\%$, similar to the 30 – 50% suggested by MR98. In addition, we investigated the effects of time-varying luminosity by parametrizing a decreasing luminosity resulting from shell expansion, and calculating the line broadening over the entire shell. For this time-dependent calculation, we included proper integration over the equal arrival time ellipse, as described by Panaiteescu and Mészáros (1998). The time-dependence does result in additional broadening, however it is not sufficient to qualitatively change our conclusions, and for simplicity we therefore employ the time-independent calculation in the results presented here. We do not include any additional broadening due to possible range of blob bulk Lorentz factors.

The density of the blobs is very high by normal astrophysical standards, and the validity of the XSTAR code under these conditions is therefore of concern. XSTAR ignores three-body recombination, assuming that the ionization equilibrium is determined by photoionization, radiation, and dielectronic recombination. Explicit calculation shows that due to the high temperatures, radiative recombination will dominate over three-body recombination, and this will not result in significant inaccuracy. A further concern is that the code does not properly treat collisional redistribution among excited levels. We estimate these errors to be at the $\sim 25 - 100\%$ level, and not of concern for reproducing gross spectral features.

Finally, we note that our results are not strongly dependent on the geometry of the entrained material. Mészáros and Rees (1998) point out that the blobs may have a filamentary structure resulting from the magnetic fields, however given our assumption of optically-thin emission, this will not significantly alter the observed spectrum.

3. RESULTS

By investigating the range of parameter space described above, we found that we could reproduce spectral features in the 10 – 100 keV band resembling the BATSE and *Ginga* measurements. Figures 1 and 2 show results from two of the best cases (i.e. those most closely resembling the broad features seen by these instruments). For each, we show the spectrum of reprocessed photons in the comoving frame, the spectrum after relativistic broadening, and the observed spectrum after convolving with the *Ginga* instrument resolution. We have not included any additional broadening due to possible spread in the blob Lorentz factors. The first case (Figure 1) has a relative abundance of metals of O:Ne:Si = 1:0.5:1, and the second (Figure 2) has O:Ne:Si:Fe = 1:0.25:0.15:0.05. The values for the ionization parameter and energy spectral index are indicated in the captions. To reproduce features with the intensity of the *Ginga* or BATSE detections requires a reprocessing rate on order unity ($\tau \sim 1$), marginally consistent with the assumption of

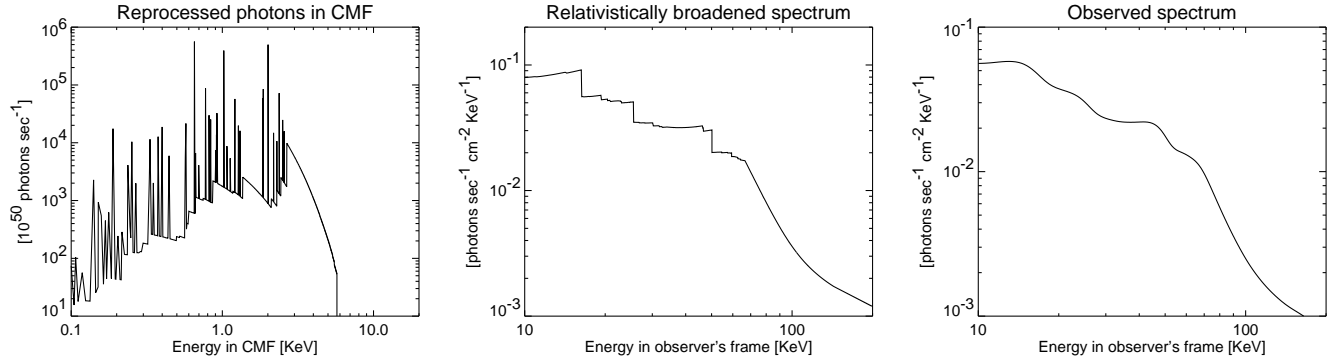


FIG. 1.— The panels, from left to right, show the spectrum of reprocessed photons in the comoving frame, the spectrum including reprocessed and continuum flux after relativistic broadening, and after convolution with a response function typical of *Ginga*. This case has a relative elemental abundance of O:Ne:Si = 1:0.5:1, $\log(\Xi) = 2.1$, a power law energy index $\alpha = 0.1$ for the ionizing flux, a plasma temperature in the comoving frame $T_{cmf} = 7.1 \times 10^6$ K, and a reprocessing rate of unity. The resulting spectrum has $\sim 2\%$ of the luminosity in the two dips between 10 - 100 keV, similar to the *Ginga* detections. For spectral normalization we have assumed $z = 1$, $\Omega = 0.2$, $H_o = 65$, and total GRB luminosity $L = 10^{51}$ erg/s.

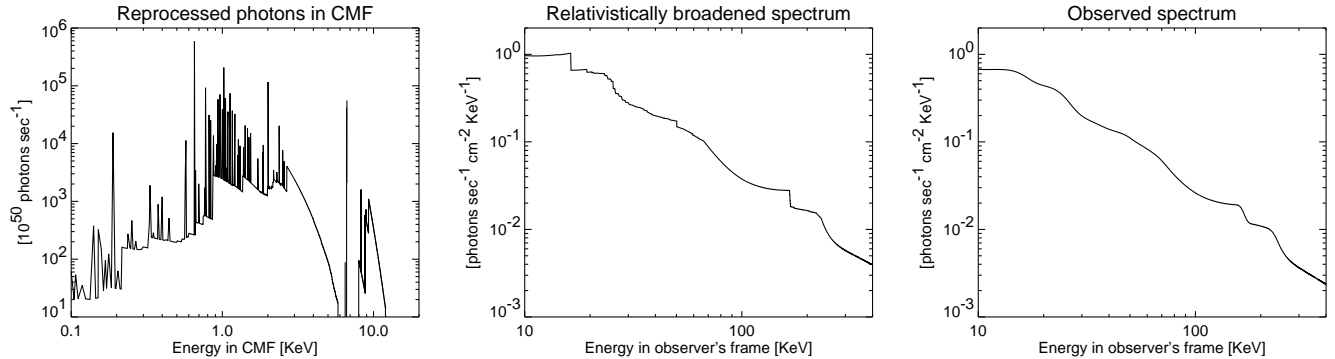


FIG. 2.— The same as in Figure 1, except that the relative metal abundance is O:Ne:Si:Fe = 1:0.25:0.15:0.05, $\log(\Xi) = 2.3$, $\alpha = 0.3$, and $T_{cmf} = 7.3 \times 10^6$ K. The two features appearing above 100 keV are due to Fe K emission (~ 150 keV) and the Fe K edge (~ 220 keV). These features could be interpreted as those observed by *ISEE*.

optically thin emission.

From Figures 1 and 2, it is clear that multiple features resembling absorption dips can be produced below 100 keV from a combination of low-Z elements, and in the case where Iron is present, from the L-shell complex. These dips, interpreted as absorption features in the *Ginga* spectra, are a result of smearing of the complex ionization structure (line emission and edges), and are not due to absorption. If the ejecta contain Iron (Figure 2), then additional emission-like features are seen in the 100 – 200 keV band due to the K-shell. Note that only one instrument has reported high-energy lines simultaneously with low-energy features. This is due primarily to instrumental limitations: reasonably large collecting area is required for high-energy detection, while good energy resolution and clean instrumental response is required below 100 keV, and these have not been combined in a single experiment. We have therefore adjusted the blob Lorentz factor to the value required to match the *Ginga* observations ($\Gamma_b = 25$) for a GRB with redshift $z = 1$. This value of the Lorentz factor is smaller than the $\Gamma_b \sim 100$ typically invoked to ensure the emission region is not opaque due to photon-photon pair production. The latter value is, however, estimated by assuming the gamma-ray spectrum extends to 100 MeV. There is no evidence for such high-energy emission in the *Ginga* events, where the low-energy line features were observed, and the value $\Gamma_b = 25$ is consistent with all the observations. Note that the 300 - 500 keV emission-like features seen in some GRB could be associated with Fe K emission edges for values of $\Gamma_b \sim 50 – 100$. Including only broadening due to the variation of velocity projected along the line of sight and typical instrumental resolution produces features consistent with the observations, while any additional broadening due to variation in blob Lorentz factors would smear out the lines entirely. We emphasize that the results presented here are the best cases, achieved by searching a fairly wide range of parameter space. For many conditions still consistent with reasonable fireball model parameters, no observable features are produced.

4. CONCLUSION

We have investigated the possibility that the 10 – 100 keV features reported in the spectra of some GRB arise from smearing of the reprocessed radiation from a metal-rich, dense photoionized plasma entrained in blobs or filaments in the relativistic outflow. By searching a relatively wide region of parameter space consistent with generic fireball models, we can reproduce the observed features for a limited set of values and elemental composition. The dips in the spectrum observed after relativistic and instrumental broadening are due to the complex ionization structure, and are a combination of emission lines and edges. In addition, the sum of the recombination spectrum plus continuum produces a break in the observed continuum at ~ 100 keV, similar to that seen by BATSE. With no additional broadening due to a range of Γ_b , relativistic effects are not sufficient to smear out the features in the recombination spectrum entirely.

If such dense, entrained blobs do exist, the broadband spectral features can be used to constrain the range of fireball model parameters, as well as the composition of the entrained material. In particular, the presence of Iron in the blobs would produce features due to K shell emission in the 100 - 1000 keV band that could be used to measure the Lorentz factor of the ejecta. We emphasize that detailed comparison with existing observations is not possible due to the uncertainties in the instrument response, and the poor signal to noise of the detections. Small variations in the response function, as well as assumed continuum, can severely alter the characteristics of the observed features (i.e. whether they are interpreted as emission or absorption dips). The primary characteristics of an experiment capable of confirming and measuring these spectral features is broad energy response (few keV – 1 MeV), large area, and clean, well-determined response function, and moderate energy resolution.

The authors wish to thank Masao Sako for assistance with XSTAR, and William Goldstein for useful discussions on the atomic physics of photoionized plasmas.

REFERENCES

Band, D. L. *et al.* 1996, ApJ, 458, 746.
 Briggs, M. S., Band, D. L., Preece, R. D., Paciesas, W. S., and Pendleton, G. N. 1999, To appear in the Proceedings of the 3rd INTEGRAL Workshop.
 Djorgovski, S. G. *et al.* 1998a, GCN notice 139.
 Djorgovski, S. G. *et al.* 1998b, ApJ, 508, L17.
 Fenimore, E. E. *et al.* 1988, ApJ, 335, L71.
 Higdon, J. C. and Lingenfelter, R. E. 1990, Ann. Rev. Astr. Ap., 28, 401.
 Hueter, G. J. 1984, in High Energy Transients in Astrophysics, ed. S. Woosley, (New York: AIP), 373.
 Kallman, T. R. and Krolik, J. H. 1995, XSTAR Manual, available via ftp at legacy.gsfc.nasa.gov.
 Kulkarni, S. R. *et al.* 1998, Nature, 393, 35.
 Kulkarni, S. R. *et al.* 1999, Nature, 397, 782.
 Liang, E. P. 1986, ApJ, 304, 682.
 Loredo, T. J. and Wasserman, I. M. 1995, ApJS, 96, 261.
 Mazets, E. P., Golenetskii, S. V., Aptekar, R. L., Guryan, Y. A., and Ilinskii, V. N. 1981, Nature, 290, 378.
 Mazets, E. P. *et al.* 1979, Nature, 282, 587.
 Mészáros, P. and Rees, M. J. 1998, ApJ, 502, L105.
 Metzger, M. R., Djorgovski, S. G., Kulkarni, S. R., Steidel, C. C., Adelberger, K. L., Frail, D. A., Costa, E., and Fronterra, F. 1997, Nature, 387, 879.
 Murakami, T. *et al.* 1988, Nature, 335, 234.
 Panaiteescu, A. and Mészáros, P. 1998, ApJ, 493, L31.
 Teegarden, B. J. and Cline, T. L. 1980, ApJ, 236, L67.